



OPEN

## SIRT1 silencing ameliorates malignancy of non-small cell lung cancer via activating FOXO1

Jiawei Chen<sup>1,3</sup>, Kebin Chen<sup>2,3</sup>, Shuai Zhang<sup>1</sup>✉ & Xiaopeng Huang<sup>1</sup>✉

Non-small cell lung cancer (NSCLC), being the most prevalent and lethal malignancy affecting the lungs, poses a significant threat to human health. This research aims at illustrating the precise role and related mechanisms of silent information regulator type-1 (SIRT1) in NSCLC progression. The expression pattern of SIRT1 in NSCLC cell lines was examined using quantitative real-time polymerase chain reaction and western blotting. Functional assays in NSCLC cell lines validated the biological capabilities of SIRT1 on malignant phenotypes, and its impact on tumorigenicity was further evaluated *in vivo*. In addition, the FOXO1 inhibitor AS1842856 was applied to verify the role of SIRT1 on FOXO pathway *in vitro*. SIRT1 expression was prominently elevated in NSCLC cell lines. The depletion of SIRT1 retarded the capabilities of proliferation, migration and invasion, while enhancing apoptosis in NSCLC cells. Furthermore, SIRT1 silencing restricted the tumorigenesis of NSCLC *in vivo*. Additionally, AS1842856 treatment ameliorated the inhibitory effect of SIRT1 deficiency on malignant phenotypes in NSCLC cells. SIRT1 deletion exerted an anti-oncogenic role in NSCLC via activation of FOXO1.

**Keywords** Non-small cell lung cancer, SIRT1, FOXO

Non-small cell lung cancer (NSCLC) accounts for 85% of lung cancer cases globally, posing high morbidity and mortality that has become a pressing societal concern<sup>1,2</sup>. Surgical resection, platinum-based doublet chemotherapy, and some targeted molecular therapies have been established as the conventional approaches for NSCLC, exhibiting advancements in recent years<sup>3</sup>. However, the outcomes of NSCLC patients remain unsatisfactory due to the limited treatment options, as reflected in the disproportionately poor overall prognosis, high recurrence rates, and the short survival time<sup>3,4</sup>. Therefore, it is of paramount importance to clarify the etiopathogenesis against NSCLC development and pinpoint more novel prospective therapeutic targets for NSCLC, which may help provide more personalized treatment options for patients with NSCLC.

Silent information regulator type-1 (SIRT1), a histone deacetylase belonging to the sirtuin family, is highly expressed in a wide spectrum of tumors, rendering it a promising therapeutic candidate target for cancer treatment<sup>5,6</sup>. For instance, SIRT1 stimulates the proliferation and metastasis of colorectal cancer cells via the p53/miR-101/KPNA3 axis<sup>7</sup>. SIRT1 modulates the CD24/Siglec-10 pathway to facilitate tumorigenesis in ovarian cancer cells<sup>8</sup>. Moreover, SNHG10/miR-543/SIRT1 axis plays as a suppressive role in the proliferation of NSCLC cells<sup>9</sup>. In addition, hsa-miR-217 targeting SIRT1/P53/KAI1 signaling restrains the tumorigenic capacity of NSCLC cells<sup>10</sup>. However, the comprehensive understanding of the molecular mechanisms underlying SIRT1 in regulation of NSCLC remains incomplete, necessitating further in-depth research.

Forkhead box O (FOXO) family consisting of four conserved transcription factors, oversees various biological processes, such as metabolism and stem cell maintenance<sup>11</sup>. Increasing vast evidence suggests that the FOXO family members are implicated in modulating cancer growth and metastasis by targeting multiple molecules<sup>12</sup>. For instance, SETD2 deletion has been found to regulate SIRT1/FOXO pathway, thereby facilitating gastric tumorigenesis<sup>13</sup>. SIRT1 possibly co-operating with FOXO proteins affects the metastasis potential of breast cancer<sup>14</sup>. SIRT1 inactivation can promote apoptosis by activating FOXO1 or p53 acetylation in lung cancer cells<sup>15</sup>. However, the correlation between SIRT1 and FOXOs in NSCLC tumorigenesis have not been elucidated to date.

Currently, the function of SIRT1 and the detailed mechanisms linked to NSCLC malignancy remain incompletely delineated. The novelty of this study lies in unveiling SIRT1 silencing retarded the tumorigenesis of

<sup>1</sup>Department of Radiation Oncology, Hainan General Hospital, Hainan Affiliated Hospital of Hainan Medical University, Haikou City 570311, Hainan Province, China. <sup>2</sup>Department of Radiation Oncology, Hainan Affiliated Hospital of Hainan Medical University, Haikou City, Hainan Province, China. <sup>3</sup>These authors contributed equally: Jiawei Chen and Kebin Chen. ✉email: 46370976@qq.com; 18976772979@163.com

NSCLC in vivo. Meanwhile, SIRT1 knockdown restrained the capabilities of proliferation, migration, and invasion, and augmented apoptosis in NSCLC cells, which was at least partially mediated by targeting FOXO1.

## Materials and methods

### Cell culture, transfection and treatment

The human bronchial epithelial cells (BEAS-2B cells) and NSCLC cell lines (A549, H1299, and Calu-1) were procured from iCell (Shanghai, China). These cells were cultivated in Dulbecco's Modified Eagle Medium (DMEM, Hyclone, Logan, UT, USA) containing 10% fetal bovine serum (FBS, Hyclone), 100 U/mL penicillin, and 100 µg/mL streptomycin (Hyclone) at 37 °C supplied with 5% CO<sub>2</sub> humidification.

To achieve SIRT1 knockdown in A549 and H1299 cells, transfection with SIRT1 siRNAs was performed. Briefly, A549 and H1299 cells were planted in 6-well plates until reaching approximately 70–80% confluency per well. Then they were transfected with 50 nM SIRT1 suppressor siRNA or a negative control (si-NC) using Lipofectamine 3000 (Invitrogen, Carlsbad, CA, USA). The transfection efficacy was assessed after 48 h of incubation. The siRNA sequences were synthesized by GenePharma (Shanghai, China) with displayed in Supplementary Table 1. In addition, H1299 cells were treated with FOXO1 inhibitor AS1842856 (1 µM, Calbiochem, Danvers, MA, USA) for further analysis.

### Quantitative real-time polymerase chain reaction (qRT-PCR)

The Trizol reagent (Invitrogen, Carlsbad, CA, USA) was used for extracting total RNA from NSCLC cell lines, followed by reversely transcribed into cDNA with PrimeScript RT Reagent kit (TaKaRa, Otsu, Japan). Afterwards, qRT-PCR analysis was conducted to determine the mRNA expression levels on the ABI7500 quantitative PCR instrument (Thermo Fisher Scientific, Waltham, MA, USA). The specific primer sequences used are provided in Supplementary Table 1. A comparative  $2^{-\Delta\Delta C_t}$  method was applied to quantify in relative expression of different samples with GAPDH acted as the reference.

### Western blot analysis

Total protein from cells was extracted, quantified, separated, and subsequently electroblotted onto polyvinylidene fluoride membranes. The membranes were then blocked with 5% skimmed milk for 2 h. After that, they were incubated at 4 °C overnight with primary antibodies against SIRT1 (ab189494, 1:1000, abcam, Cambridge, UK), FOXO1 (ab131339, 1:1000, abcam), and GAPDH (5174, 1:1000, Cell Signaling Technology, Danvers, MA, USA). Following incubation with HRP-conjugated secondary antibodies, the immunoblots were visualized utilizing imager system (Bio-Rad, Hercules, CA, USA) with GAPDH served as an endogenous control, and the intensity of the western bands was quantified by ImageJ software (V1.8.0.112, NIH, Madison, WI, USA).

### Cell counting kit- 8 (CCK-8) assay

Briefly, the cells ( $1 \times 10^3$  cells/well) were seeded onto a 96-well plate and cultured in complete DMEM medium for 0, 24, 48, 72 and 96 h at 37 °C incubator, then CCK-8 working solution (Beyotime, Shanghai, China) was added to incubate the cells for additional 2 h. The absorbance at the wavelength of 450 nm was detected with a microplate reader (VL0000D0, Thermo Fisher Scientific).

### EdU assay

Briefly, cells ( $1 \times 10^5$  cells/well) were seeded in 24-well plates until the cells reached 70–80% confluence, and then 20 µM of 5-ethynyl-2'-deoxyuridine (EdU) working solution (Beyotime) were added to each well. Subsequently, the labelled cells were fixed, permeabilized, and exposed to 4', 6-diamidino-2-phenylindole (DAPI) solution for staining the nuclei. Finally, the EdU-positive cells were observed under a fluorescence microscope (Leica Microsystems GmbH, Wetzlar, Germany).

### Flow cytometry analysis

The cells were grown in 6-well plates at a density of  $5 \times 10^5$  cells per well and maintained at 37 °C for 24 h. After different treatment, the cells were collected, washed, and resuspended in a binding buffer, followed by staining with 5 µL AnnexinV-FITC/PI (Beyotime) for 15 min in the dark. Finally, apoptosis was measured by flow cytometry (BD Biosciences, San Jose, CA, USA).

### Wound healing assay

To validate cell migration using the wound-healing assay, A549 and H1299 cells were seeded ( $5 \times 10^5$ /well) in 6-well plates until the forming a confluent monolayer. A mechanical scratch was generated with a pipette tip in the cell layer, and the cells were then cultivated in serum-free medium for 24 h at 37 °C. Images of the wound were captured at both 0 and 24 h using microscopy (Olympus). Finally, the migration distance was determined with ImageJ software, and migration rate was calculated based on the following formula: migration rate = (0 h scratch width – 24 h scratch width) / (0 h scratch width) × 100%.

### Transwell assay

The NSCLC cells ( $2 \times 10^4$  cells) suspended in serum-free DMEM medium were seeded into the upper chamber, which had been pre-coated with Matrigel (BD Biosciences, San Jose, CA). Meanwhile, the lower chamber was filled with medium containing 20% FBS, serving as a chemoattractant. After incubation for 24 h at 37 °C, the non-invading cells on the upper surface of the filter were gently wiped off with cotton swabs. Cells that attached

to the underside of well were then fixed in 4% paraformaldehyde, dyed with 0.2% crystal violet and counted using microscopy (Olympus).

### Bioinformatics analysis

The intersecting genes between genes related to NSCLC and genes co-expressed with SIRT1 were screened using the GeneCards (<https://www.genecards.org/>) and CoxPresdb (<https://coxpresdb.jp/>) databases. Subsequently, the Kyoto Encyclopedia of Genes and Genome (KEGG) pathway enrichment analysis was carried out on the Database for Annotation, Visualization and Integrated Discovery (DAVID, <https://david.ncicrf.gov/summary.jsp>) tool<sup>16–18</sup>.

### In vivo investigations

Silencing of SIRT1 (lv-SIRT1) and negative controls (lv-NC) were constructed through the lentivirus-based vectors by GenePharma (Shanghai, China). A total of twelve male BALB/c nude mice (6–8 week-old, weighing 18–20 g) were purchased from SPF Biotechnology Co., Ltd. (Beijing, China) and randomly allocated into two groups: lv-NC and lv-SIRT1 (n = 6 per group). The A549 cells ( $2 \times 10^6$ ) transfected with either lv-NC or lv-SIRT1 were subcutaneously injected into the right armpit of each mice to establish an NSCLC tumor model. The tumor size of the mice was recorded every 7 days with computed using the formula:  $V = (\text{length} \times \text{width}^2)/2$ . On the 28th day after transplantation, all the mice were euthanized through inhalation of isoflurane (Rayward, Shenzhen, China) for 2–3 min. The complete tumors were excised and weighted. All the experimental protocols were approved by the Animal Care and Use Committee of Hainan General Hospital, Hainan Affiliated Hospital of Hainan Medical University (approval number: No. 2021-265).

### Hematoxylin and eosin (HE) staining

The tissues were fixed in 4% paraformaldehyde solution, followed by gradient dehydration, paraffin-embedded procedures, and then cut into slices. After the slices were dewaxed with xylene, the sections were stained with hematoxylin and counterstained with eosin solution, then were sealed with neutral gum. Finally, the images were captured under a microscope (Olympus).

### Immunohistochemistry (IHC)

Briefly, tumor tissues were fixed, embedded in paraffin, and sliced into 4  $\mu\text{m}$  sections. Afterwards, the paraffin-embedded specimens underwent deparaffinization and rehydration and then were heated in citrate buffer. After inactivation with 3% hydrogen peroxide, the tissue slides were incubated overnight at 4 °C with antibodies against Ki67 (ab15580, 1:1000, abcam), SIRT1 (ab189494, 1:500, abcam) and FOXO1 (ab131339, 1:100, abcam), then dyed with the 3, 3'-diaminobenzidine solution (DAB, zli-9018; zsbio, Beijing, China), re-stained with hematoxylin, and sealed. Finally, the sections were photographed under microscopy (Olympu).

### Statistical analysis

Each experiment was carried out at least three independent replicates and the quantitative data were represented as the mean  $\pm$  standard deviation using GraphPad Prism 9.0 (GraphPad Software Inc., San Diego, CA, USA). Student's t-test was applied to evaluate differences between the two groups, while one-way ANOVA, coupled with Tukey's test, was used for analyzing differences among multiple groups. A *p* value < 0.05 was considered as statistical significance.

### Ethics approval and consent to participate

The experiments conformed to the Guide for the Care and Use of Laboratory Animals. Animal study has been approved by the Animal Ethics Committee of Hainan 14 General Hospital, Hainan Affiliated Hospital of Hainan Medical University (No. 2021-265). All methods are reported in accordance with ARRIVE guidelines.

## Results

### SIRT1 silencing suppresses proliferation and promotes apoptosis of NSCLC cells

To explore the expression pattern of SIRT1, we initially evaluated its expression in BEAS-2B and NSCLC cell lines. Compared with BEAS-2B cells, the expression of SIRT1 was remarkably elevated at both mRNA and protein levels in A549, H1299, and Calu-1 cells (Fig. 1A). SIRT1 knockdown was achieved by transfection with SIRT1 siRNAs, resulting in a noticeable reduction in SIRT1 expression in both A549 and H1299 cells, as compared to the si-NC group, then si-SIRT1-1 and si-SIRT1-2 were selected for further experiments (Fig. 1B). SIRT1 knockdown significantly suppressed the viability and proliferation ability of both A549 and H1299 cells compared to the si-NC group (Fig. 1C–D). Furthermore, the number of apoptotic cells was significantly increased in the si-SIRT1s group (Fig. 1E). Collectively, SIRT1 deletion could suppress proliferation and augment apoptosis in NSCLC cells.

### SIRT1 knockdown blocks the migration and invasion of NSCLC cells

We next checked the impact of SIRT1 knockdown on the migration and invasion abilities of NSCLC cells. The results revealed that SIRT1 deficiency led to inhibition of migratory capabilities of both A549 and H1299 cells (Fig. 2A). Moreover, SIRT1 silencing led to a marked reduction in the invasive processes of NSCLC cells (Fig. 2B). These results indicated that SIRT1 downregulation restrained migrating and invading capabilities of NSCLC cells.

### Downregulation of SIRT1 attenuates tumorigenicity of NSCLC in vivo

For further exploring the impact of SIRT1 on tumor growth, a tumorigenesis model was established. The mice in lv-SIRT1 group, exhibited lighter tumor weight and smaller tumor volume compared to those in lv-NC group

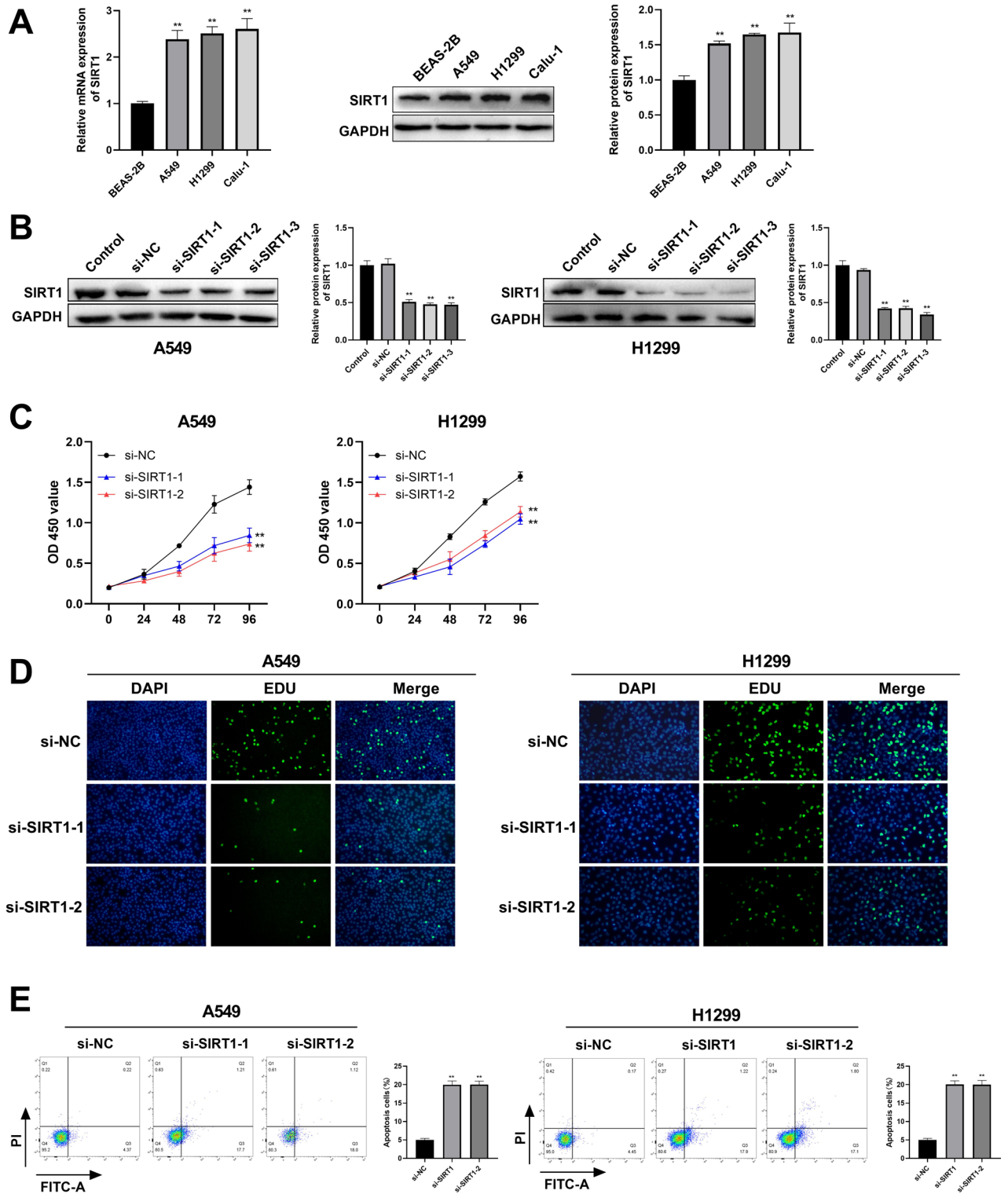


**Fig. 1.** SIRT1 silencing suppresses proliferation and promotes apoptosis of NSCLC cells. (A) The expression of SIRT1 at mRNA and protein levels in A549, H1299, and Calu-1 cells. (B) The silencing efficiency of SIRT1 was determined using qRT-PCR and western blot technique. (C) The CCK-8 assay was used to measure the viability of A549 and H1299 cells in the si-NC and si-SIRT1s groups. (D) The proliferation of A549 and H1299 cells in the si-NC and si-SIRT1s groups was evaluated using the EdU assay. (E) Apoptosis of NSCLC cells in each group was detected by flow cytometry. \*\**p* < 0.01 vs. si-NC.

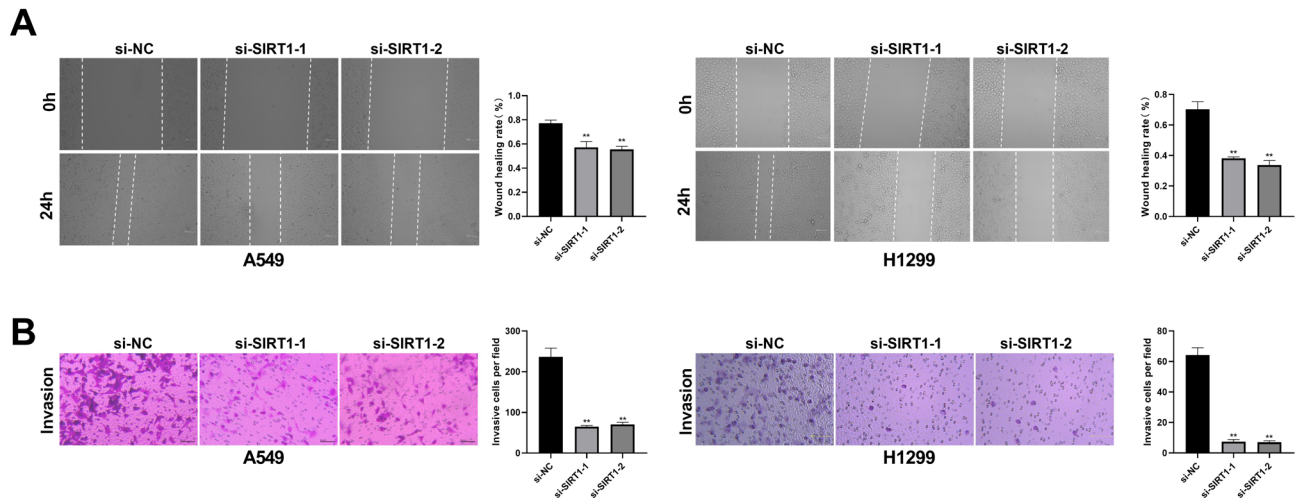


**Fig. 2.** SIRT1 knockdown blocks the migration and invasion of NSCLC cells. **(A)** Wound-healing assay was conducted to detect cell migration in NSCLC cell lines characterized by knockdown of SIRT1. Scale bar: 100  $\mu$ m. **(B)** To assess the effect of SIRT1 silencing on NSCLC cell invasion, the transwell assay was conducted. Scale bar: 100  $\mu$ m. \*\* $p < 0.01$  vs. si-NC.

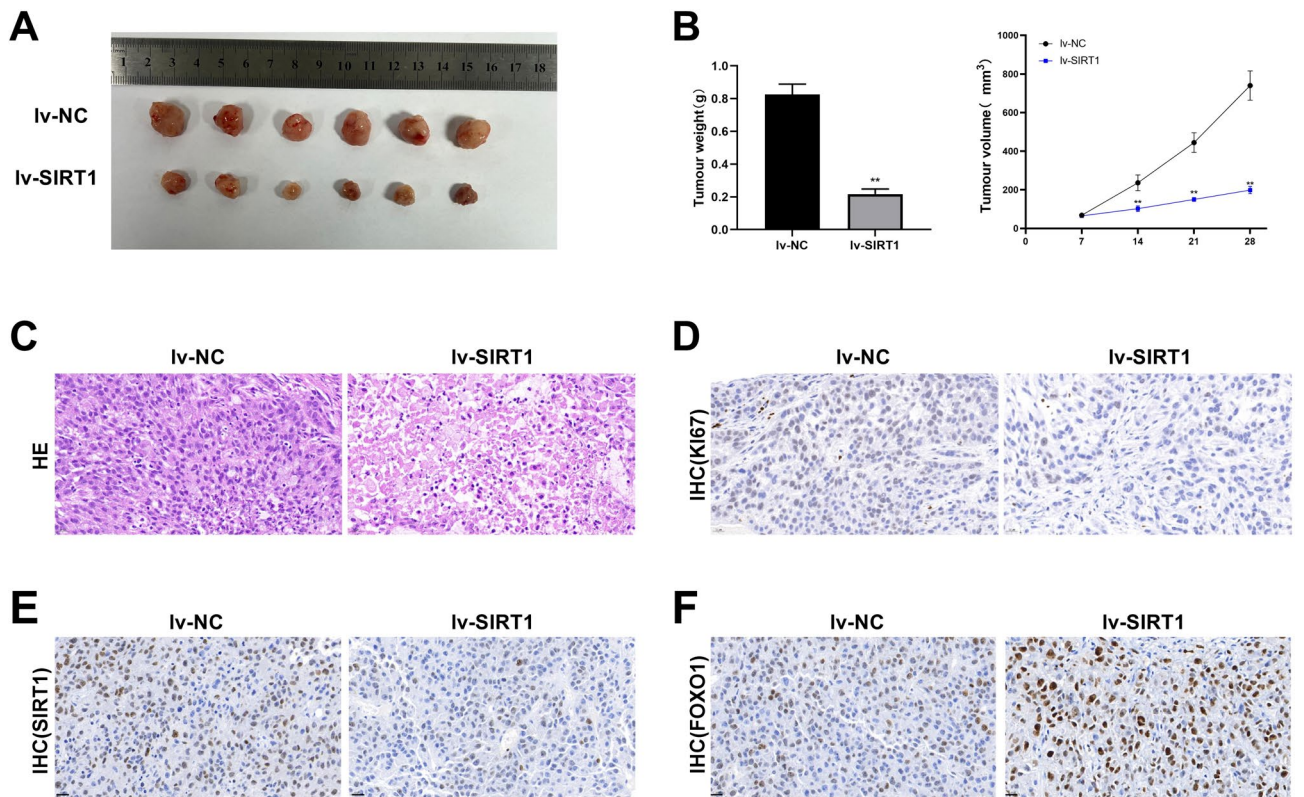


**Fig. 3.** Downregulation of SIRT1 attenuates tumorigenicity of NSCLC in vivo. **(A)** Representative image of the tumors harvested from the Iv-NC and Iv-SIRT1 group (n = 6). **(B)** Tumor weight was compared between two groups. The tumor volume growth curves of each group were determined. **(C)** HE staining was used to detect the pathological changes in tumors. Amplification: 400 $\times$ , scale bar: 20  $\mu$ m. **(D)** IHC images of Ki-67 in each group. Amplification: 400 $\times$ , scale bar: 20  $\mu$ m. **(E)** IHC staining of SIRT1 expression in tumor tissues of Iv-NC and Iv-SIRT1 groups. Amplification: 400 $\times$ , scale bar: 20  $\mu$ m. **(F)** IHC staining of FOXO1 expression in tumor tissues of Iv-NC and Iv-SIRT1 groups. Amplification: 400 $\times$ , scale bar: 20  $\mu$ m. \*\* $p < 0.01$  vs. Iv-NC.

(Fig. 3A–B). Besides, downregulation of SIRT1 remarkably reduced tumor malignancy (Fig. 3C). In addition, the number of the Ki-67 and SIRT1 positive cells was decreased in SIRT1-silenced tissues by immunohistochemistry (Fig. 3D–E). Taken together, SIRT1 depletion could significantly attenuate tumorigenicity of NSCLC *in vivo*.

### Inhibition of SIRT1 is correlated with FOXO pathway activation in NSCLC cells

To further dissect the potential pathway mediated by SIRT1 in the development of NSCLC, we applied database GeneCards and Coxpresdb to screen intersected genes between genes related to NSCLC and co-expressed genes with SIRT1, and 299 genes were extracted (Fig. 4A). Subsequently, the KEGG enrichment analysis illustrated that these overlapping genes were primarily participated in the FOXO signaling pathway, TGF- $\beta$  pathway, and Hippo pathway (Fig. 4B). We then further focused on the effect of SIRT1 on the FOXO signaling pathway. The expression of FOXO1 in SIRT1-silenced tumor tissues and NSCLC cells was remarkably elevated (Fig. 3F, Fig. 4C). Furthermore, the mRNA expression level of FOXO3 was increased in A549 and H1299 cells after SIRT1 silencing (Fig. 4D). These data implied that SIRT1 deletion may be involved in regulating the expression of molecules related to FOXO pathway.

### SIRT1 deletion restrains the malignant phenotypes of NSCLC cells by targeting FOXO1

To further determine whether SIRT1 deletion restrained the malignant phenotypes of NSCLC cells (H1299 cells) by targeting FOXO1, FOXO1 inhibitor AS1842856, was employed. Treatment with AS1842856 reversed the increase in FOXO1 mRNA expression in H1299 cells after SIRT1 silencing (Fig. 5A). Additionally, AS1842856 attenuated the inhibitory effect of SIRT1 silencing on cell viability and proliferation capacity (Fig. 5B–C). Furthermore, the rate of apoptosis was lower in the si-SIRT1 + AS1842856 group than that in the si-SIRT1 group (Fig. 5D). In addition, suppression of SIRT1 in migration and invasion could be blocked by AS1842856 treatment

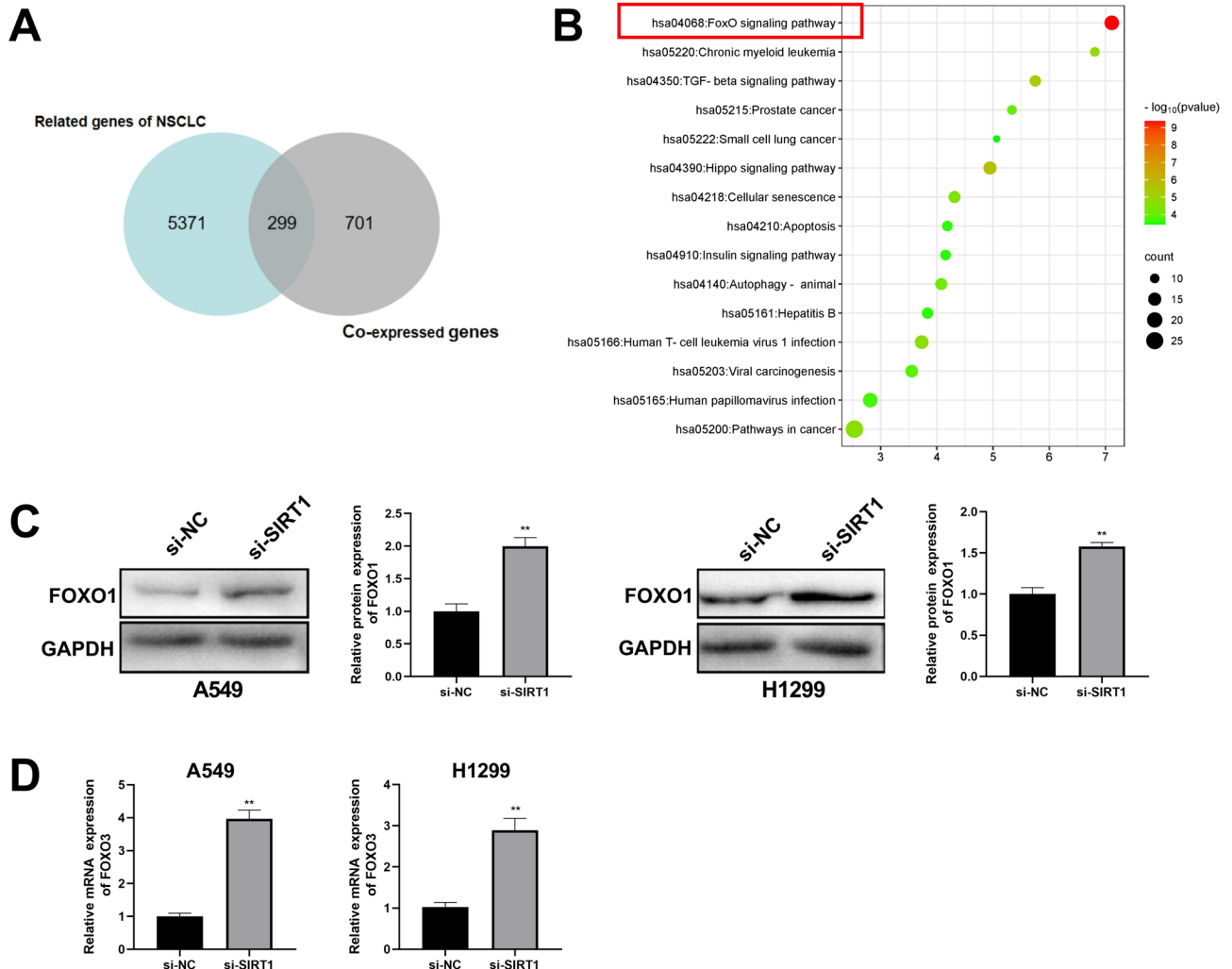


**Fig. 4.** Inhibition of SIRT1 is correlated with FOXO pathway activation in NSCLC cells. **(A)** Venn diagram of SIRT1 co-expressed genes and NSCLC-associated genes. **(B)** KEGG functional enrichment analysis of intersected genes. **(C)** FOXO1 protein expression of each group in A549 and H1299 cells were detected by western blot. **(D)** FOXO3 mRNA expression of each group in A549 and H1299 cells were determined. \*\* $p < 0.01$  vs. si-NC.

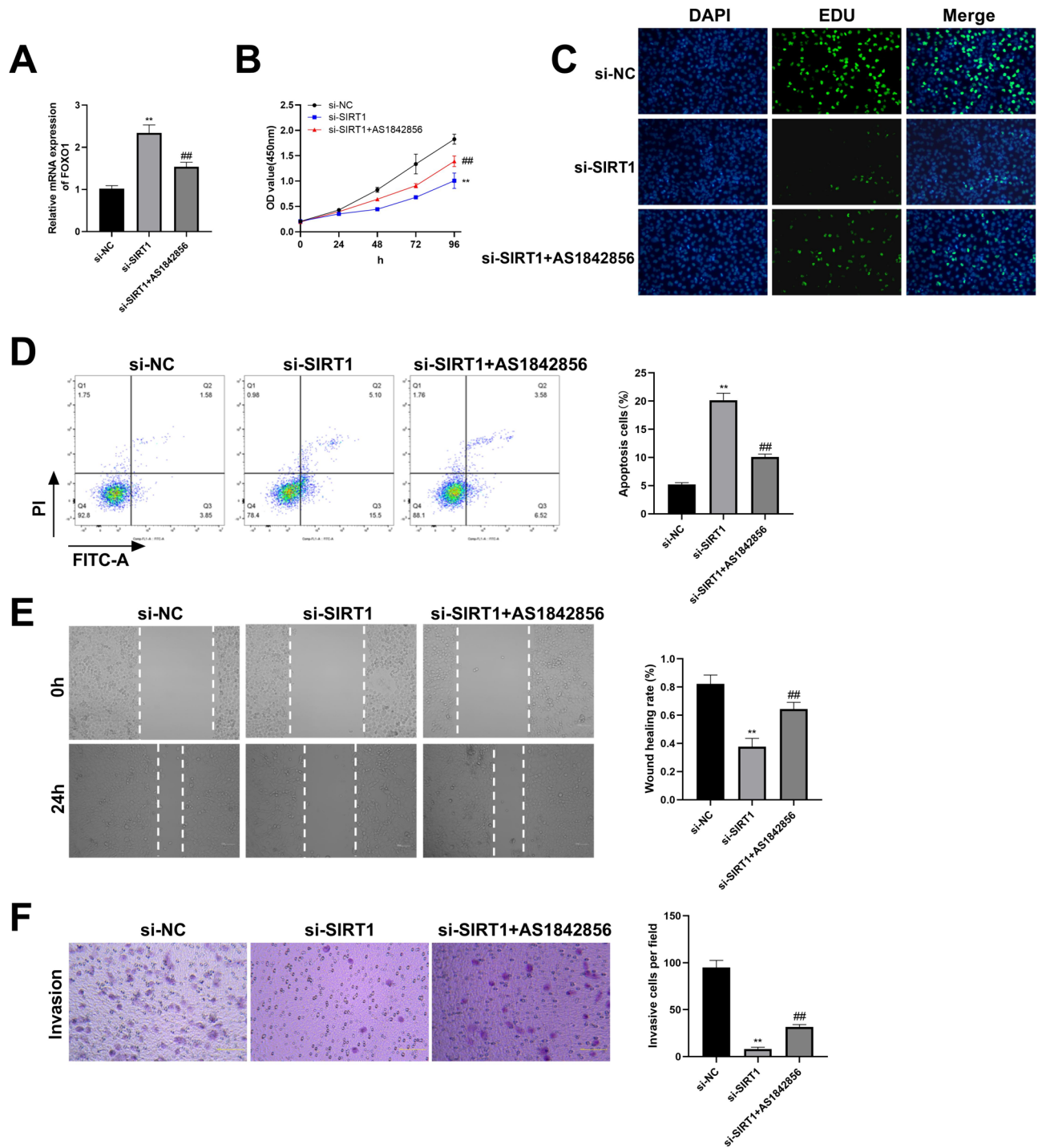


**Fig. 5.** SIRT1 deletion restrains the malignant phenotypes of NSCLC cells via FOXO pathway. (A) The expression levels of FOXO1 in H1299 cells after SIRT1 interference and subsequent AS1842856 treatment were checked by qRT-PCR. (B) The viability of H1299 cells after different treatment was measured by CCK-8. (C) EDU assay for the assessment of the cell proliferation in H1299 cells after different treatment. (D) The apoptosis of NSCLC cells in each group was assessed through flow cytometry. (E) The migration of NSCLC cells in each group was measured using the wound healing assay. Scale bar: 100  $\mu$ m. (F) The invasion ability of NSCLC cells stably in each group was detected by transwell assay. Scale bar: 100  $\mu$ m. \*\* $p$  < 0.01 vs. si-NC; ## $p$  < 0.01 vs. si-SIRT1.

(Fig. 5E–F). Thus, these results revealed that SIRT1 deletion attenuated malignant phenotypes in NSCLC cells by targeting FOXO1.

## Discussion

NSCLC is the most prevalent and lethal type of lung cancer with a high metastatic spread rate but limited treatment options that has posed a severe threat to human health<sup>19,20</sup>. Hence, further elucidating the crucial mechanisms involved in the pathogenesis of NSCLC and digging out more appropriate perspective targets is crucial for effective NSCLC treatment. In this study, our results demonstrate that SIRT1 silencing attenuated malignant phenotypes of NSCLC cell lines and impeded tumorigenesis *in vivo*, which were mediated by the mechanism involved in activating FOXO1.

SIRT1, an essential regulator, is participated in modulating apoptosis, proliferation, aging, and carcinogenesis<sup>21</sup>. Previous studies have shown that downregulation of SIRT1 can target p53 to suppress ferroptosis, thereby facilitating the growth of gastric cancer cells<sup>22</sup>. Besides, SIRT1 silencing is able to aggravate cell death in glioma<sup>23</sup>. Furthermore, SIRT1 deficiency has the ability to restrain malignant phenotypes in aggressive colorectal cancer cells and also to repress colorectal cancer metastasis *in vivo*<sup>24</sup>. SIRT1 depletion also exhibits the inhibitory effects on capabilities of proliferation and colony formation of T-cell acute lymphoblastic leukemia cells, and can prolong the survival time of T-cell acute lymphoblastic leukemia model mice<sup>25</sup>. In addition, SIRT1 knockdown plays an anti-oncogenic role in breast cancer, reflected by a decrease in the proliferative, migratory, and invasive capacities of human breast cancer cells<sup>26</sup>. Consistently, in the present study, the mRNA and protein expression levels of SIRT1 were both apparently elevated in NSCLC cell lines. Furthermore, SIRT1 deletion was able to retard the proliferation, migration and invasion, as well as to augment apoptosis of NSCLC cells. In addition, downregulation of SIRT1 also restricted tumorigenesis of NSCLC *in vivo*.

Reactivation of FOXO pathway represents a promising emerging therapy option for cancer conditions. For instance, knockdown of KPNA2 suppresses cell viability, migration rate and invasion capacity of laryngeal cancer cells by enhancing ferroptosis through activation of the FOXO signaling pathway<sup>27</sup>. Moreover, the combination of FTO and ALKBH5 knockdown activates the FOXO signaling pathway, leading to enhanced proliferative capability in colorectal cancer cells<sup>28</sup>. Similarly, SUV39H2 deficiency significantly impedes the growth of prostate cancer cells, mediated by AKT/FOXO signaling pathway<sup>29</sup>. Moreover, miR-96-5p directly interacts with FOXO3 to accelerate cell proliferation in gastric cancer<sup>30</sup>. Furthermore, MicroRNA-27a-3p knockout delays tumor behavior and growth in cholangiocarcinoma by increasing the FOXO1 levels<sup>31</sup>. In addition, RhoC deletion can restrain M2 macrophage polarization through in regulation of PTEN/FOXO1 pathway, thereby reducing malignant phenotypes of colon cancer cells and tumorigenesis in mice tumor model<sup>32</sup>. Herein, we found that SIRT1 deficiency was correlated with FOXO activation in NSCLC cells, as evidenced by the increase in FOXO1 mRNA and protein expression levels. Meanwhile, the mRNA expression level of FOXO3 was also elevated in SIRT1-silenced NSCLC cells. Moreover, our results elucidated that FOXO1 inhibitor AS1842856 treatment attenuated the inhibitory effect of SIRT1 silencing on proliferative, migratory and invasive capabilities, and also restrained the pro-apoptotic effect in NSCLC cells.

As our KEGG analysis suggests, in addition to the FOXO pathway, the intersected genes share between NSCLC-related genes and co-expressed genes with SIRT1 are also participated in TGF- $\beta$  and Hippo pathway. MiR-20a targeting RUNX3 exacerbates the malignant progression of NSCLC by activating the TGF- $\beta$  signaling pathway<sup>33</sup>. TRIM66 serves as a carcinogenic role in the tumor genesis and development of NSCLC, which is modulated via TGF- $\beta$ /SMAD pathway<sup>34</sup>. Furthermore, ACTL6A facilitates the proliferation in NSCLC, which is mediated by the Hippo/YAP pathway<sup>35</sup>. Through YAP expression regulation and Hippo pathway inactivation, ANKHD1 hastens the invasion and proliferation of NSCLC cells<sup>36</sup>. In addition, WBP2 accelerates the tumorigenicity of NSCLC by negatively regulating the Hippo pathway via competitive binding to WWC3-LATS1<sup>37</sup>. Nonetheless, further investigations are essential so as to further illustrate crosstalk between SIRT1 and TGF- $\beta$  or Hippo pathway in the development of NSCLC.

However, this research has several limitations. Firstly, we have preliminarily explored the potential pathways mediated by SIRT1 in NSCLC development using bioinformatics alone, which RNA-seq should be further performed to confirm the discovered signaling pathway participated. Secondly, due to the difficulties in obtaining suitable clinical samples, the functional effects of SIRT1 silencing on NSCLC were only demonstrated in cellular and animal investigations rather than being clinically verified. Thirdly, the downstream genes regulated by FOXO1 should be further comprehensively investigated in the future. Additionally, although SIRT1 knockdown exhibited profound effects on ameliorating malignancy NSCLC, incorporating SIRT1 overexpression would further strengthen the persuasiveness of the findings.

To summarize, our findings illustrated that SIRT1 was highly expressed in NSCLC cell lines. Downregulation of SIRT1 could repress the malignant phenotypes of NSCLC cell lines and retard tumorigenesis *in vivo*. Mechanistically, SIRT1 deletion mitigated malignancy of NSCLC via activation of FOXO1. Collectively, the findings of this study offer an essential theoretical basis, highlighting SIRT1 deficiency as a novel and promising candidate target for the treatment of NSCLC.

## Data availability

The datasets used and/or analysed during the current study are available from the corresponding author on reasonable request.

Received: 10 May 2024; Accepted: 22 August 2024

Published online: 28 August 2024

## References

1. Relli, V., Trerotola, M., Guerra, E. & Alberti, S. Abandoning the notion of non-small cell lung cancer. *Trends Mol. Med.* **25**(7), 585–594. <https://doi.org/10.1016/j.molmed.2019.04.012> (2019).



2. Kaur, J., Elms, J., Munn, A. L., Good, D. & Wei, M. Q. Immunotherapy for non-small cell lung cancer (NSCLC), as a stand-alone and in combination therapy. *Crit. Rev. Oncol. Hematol.* **164**, 103417. <https://doi.org/10.1016/j.critrevonc.2021.103417> (2021).
3. Singh, T. & Fatehi Hassanabad, M. Fatehi Hassanabad A (2021) Non-small cell lung cancer: Emerging molecular targeted and immunotherapeutic agents. *Biochim. Biophys. Acta* **2**, 188636. <https://doi.org/10.1016/j.bbcan.2021.188636> (1876).
4. Chen, R. *et al.* Emerging therapeutic agents for advanced non-small cell lung cancer. *J. Hematol. Oncol.* **13**(1), 58. <https://doi.org/10.1186/s13045-020-00881-7> (2020).
5. Shen, S. *et al.* SIRT1/SREBPs-mediated regulation of lipid metabolism. *Pharmacol. Res.* **199**, 107037. <https://doi.org/10.1016/j.phrs.2023.107037> (2024).
6. Zhao, B., Li, X., Zhou, L., Wang, Y. & Shang, P. SIRT1: a potential tumour biomarker and therapeutic target. *J. Drug Target.* **27**(10), 1046–1052. <https://doi.org/10.1080/1061186x.2019.1605519> (2019).
7. Wang, X. W. *et al.* SIRT1 promotes the progression and chemoresistance of colorectal cancer through the p53/miR-101/KPNA3 axis. *Cancer Biol. Ther.* **24**(1), 2235770. <https://doi.org/10.1080/15384047.2023.2235770> (2023).
8. Zheng, Q. *et al.* Delivery of SIRT1 by cancer-associated adipocyte-derived extracellular vesicles regulates immune response and tumorigenesis of ovarian cancer cells. *Clin. Transl. Oncol. Off. Publ. Federation Spanish Oncol. Soc. National Cancer Ins. Mexico* **26**(1), 190–203. <https://doi.org/10.1007/s12094-023-03240-3> (2024).
9. Zhang, Z. *et al.* Long noncoding RNA SNHG10 sponges miR-543 to upregulate tumor suppressive sirt1 in nonsmall cell lung cancer. *Cancer Biother. Radiopharm.* **35**(10), 771–775. <https://doi.org/10.1089/cbr.2019.3334> (2020).
10. Jiang, W. *et al.* Hsa-miR-217 inhibits the proliferation, migration, and invasion in non-small cell lung cancer cells via targeting SIRT1 and P53/KAI1 signaling. *Balkan Med. J.* **37**(1), 208–214. <https://doi.org/10.4274/balkanmedj.galenos.2020.2019.9.91> (2020).
11. Liu, Y. *et al.* The FOXO family of transcription factors: key molecular players in gastric cancer. *J. Mol. Med. (Berl)* **100**(7), 997–1015. <https://doi.org/10.1007/s00109-022-02219-x> (2022).
12. Farhan, M. *et al.* The role of FOXOs and autophagy in cancer and metastasis-Implications in therapeutic development. *Med. Res. Rev.* **40**(6), 2089–2113. <https://doi.org/10.1002/med.21695> (2020).
13. Feng, W. *et al.* Setd2 deficiency promotes gastric tumorigenesis through inhibiting the SIRT1/FOXO pathway. *Cancer Lett.* **579**, 216470. <https://doi.org/10.1016/j.canlet.2023.216470> (2023).
14. Dilmac, S. *et al.* SIRT1/FOXO signaling pathway in breast cancer progression and metastasis. *Int. J. Molecular Sci.* <https://doi.org/10.3390/ijms231810227> (2022).
15. Zhang, Y. *et al.* S-nitrosylation of the Peroxiredoxin-2 promotes S-nitrosoglutathione-mediated lung cancer cells apoptosis via AMPK-SIRT1 pathway. *Cell Death Dis.* **10**(5), 329. <https://doi.org/10.1038/s41419-019-1561-x> (2019).
16. Kanehisa, M. & Goto, S. KEGG: kyoto encyclopedia of genes and genomes. *Nucleic Acids Res.* **28**(1), 27–30. <https://doi.org/10.1093/nar/28.1.27> (2000).
17. Kanehisa, M. Toward understanding the origin and evolution of cellular organisms. *Protein Sci. Publ. Protein Soc.* **28**(11), 1947–1951. <https://doi.org/10.1002/pro.3715> (2019).
18. Kanehisa, M., Furumichi, M., Sato, Y., Kawashima, M. & Ishiguro-Watanabe, M. KEGG for taxonomy-based analysis of pathways and genomes. *Nucleic Acids Res.* **51**(D1), D587–d592. <https://doi.org/10.1093/nar/gkac963> (2023).
19. Li, S. *et al.* Targeted therapy for non-small-cell lung cancer: New insights into regulated cell death combined with immunotherapy. *Immunol. Rev.* **321**(1), 300–334. <https://doi.org/10.1111/immr.13274> (2024).
20. Liang, S., Zhou, G. & Hu, W. Research progress of heavy ion radiotherapy for non-small-cell lung cancer. *Int. J. Molecular Sci.* <https://doi.org/10.3390/ijms23042316> (2022).
21. Jiang, Y. Z., Huang, X. R., Chang, J., Zhou, Y. & Huang, X. T. SIRT1: An intermedator of key pathways regulating pulmonary diseases. *Lab. Investig. J. Techn. Methods Pathol.* **104**(5), 102044. <https://doi.org/10.1016/j.labinv.2024.102044> (2024).
22. Zhao, H., Ding, Y. & Zhang, L. SIRT1/APE1 promotes the viability of gastric cancer cells by inhibiting p53 to suppress ferroptosis. *Open Med. (Warsaw, Poland)* **18**(1), 20220620. <https://doi.org/10.1515/med-2022-0620> (2023).
23. Chen, X. *et al.* SIRT1 activated by AROS sensitizes glioma cells to ferroptosis via induction of NAD<sup>+</sup> depletion-dependent activation of ATF3. *Redox Biol.* **69**, 103030. <https://doi.org/10.1016/j.redox.2024.103030> (2024).
24. Cheng, F. *et al.* SIRT1 promotes epithelial-mesenchymal transition and metastasis in colorectal cancer by regulating Fra-1 expression. *Cancer Lett.* **375**(2), 274–283. <https://doi.org/10.1016/j.canlet.2016.03.010> (2016).
25. Wang, F. *et al.* SIRT1 regulates the phosphorylation and degradation of P27 by deacetylating CDK2 to promote T-cell acute lymphoblastic leukemia progression. *J. Exp. Clin. Cancer Res.* **CR** **40**(1), 259. <https://doi.org/10.1186/s13046-021-02071-w> (2021).
26. Xu, Y., Qin, Q., Chen, R., Wei, C. & Mo, Q. SIRT1 promotes proliferation, migration, and invasion of breast cancer cell line MCF-7 by upregulating DNA polymerase delta1 (POLD1). *Biochem. Biophys. Res. Commun.* **502**(3), 351–357. <https://doi.org/10.1016/j.bbrc.2018.05.164> (2018).
27. Xu, M., Hu, X., Xiao, Z., Zhang, S. & Lu, Z. Silencing KPNA2 promotes ferroptosis in laryngeal cancer by activating the FoxO signaling pathway. *Biochem. Genet.* <https://doi.org/10.1007/s10528-023-10655-8> (2024).
28. Ye, M. *et al.* Down-regulated FTO and ALKBH5 co-operatively activates FOXO signaling through m6A methylation modification in HK2 mRNA mediated by IGF2BP2 to enhance glycolysis in colorectal cancer. *Cell Biosci.* **13**(1), 148. <https://doi.org/10.1186/s13578-023-01100-9> (2023).
29. Sun, D. *et al.* Histone methyltransferase SUV39H2 regulates apoptosis and chemosensitivity in prostate cancer through AKT/FOXO signaling pathway. *Med. Oncol. (Northwood, London, England)* **41**(2), 44. <https://doi.org/10.1007/s12032-023-02252-x> (2024).
30. He, X. & Zou, K. MiRNA-96-5p contributed to the proliferation of gastric cancer cells by targeting FOXO3. *J. Biochem.* **167**(1), 101–108. <https://doi.org/10.1093/jb/mvz080> (2020).
31. Duwe, L. *et al.* MicroRNA-27a-3p targets FoxO signalling to induce tumour-like phenotypes in bile duct cells. *J. Hepatol.* **78**(2), 364–375. <https://doi.org/10.1016/j.jhep.2022.10.012> (2023).
32. Yang, B., Wang, L. & Tian, Z. Silencing of RhoC induces macrophage M1 polarization to inhibit migration and invasion in colon cancer via regulating the PTEN/FOXO1 pathway. *Int. J. Exp. Pathol.* **104**(1), 33–42. <https://doi.org/10.1111/iep.12460> (2023).
33. Qin, X. *et al.* MiR-20a promotes lung tumorigenesis by targeting RUNX3 via TGF-beta signaling pathway. *J. Biol. Regul. Homeostatic Agents* <https://doi.org/10.23812/20-12a> (2020).
34. Chen, W., Zhang, Y., Fang, Z., Qi, W. & Xu, Y. TRIM66 hastens the malignant progression of non-small cell lung cancer via modulating MMP9-mediated TGF-beta/SMAD pathway. *Cytokine* **153**, 155831. <https://doi.org/10.1016/j.cyto.2022.155831> (2022).
35. Ma, L. & Shan, L. ACTL6A promotes the growth in non-small cell lung cancer by regulating Hippo/Yap pathway. *Exp. Lung Res.* **47**(5), 250–259. <https://doi.org/10.1080/01902148.2021.1916651> (2021).
36. Liu, X. F. *et al.* ANKHD1 promotes proliferation and invasion of nonsmallcell lung cancer cells via regulating YAP oncoprotein expression and inactivating the Hippo pathway. *Int. J. Oncol.* **56**(5), 1175–1185. <https://doi.org/10.3892/ijo.2020.4994> (2020).
37. Han, Q. *et al.* WBP2 negatively regulates the Hippo pathway by competitively binding to WWC3 with LATS1 to promote non-small cell lung cancer progression. *Cell Death Dis.* **12**(4), 384. <https://doi.org/10.1038/s41419-021-03600-3> (2021).

## Author contributions

Jiawei Chen and Kebin Chen: Conceptualization; Formal analysis; Methodology; Writing—original draft; Validation; Resources; Shuai Zhang and Xiaopeng Huang: Formal analysis; Methodology; Validation; all authors have read and approved the manuscript.

### Funding

This work was supported by Natural Science Foundation of Hainan Province (No. 822QN460).

### Competing interests

The authors declare no competing interests.

### Additional information

**Supplementary Information** The online version contains supplementary material available at <https://doi.org/10.1038/s41598-024-70970-x>.

**Correspondence** and requests for materials should be addressed to S.Z. or X.H.

**Reprints and permissions information** is available at [www.nature.com/reprints](http://www.nature.com/reprints).

**Publisher's note** Springer Nature remains neutral with regard to jurisdictional claims in published maps and institutional affiliations.

**Open Access** This article is licensed under a Creative Commons Attribution-NonCommercial-NoDerivatives 4.0 International License, which permits any non-commercial use, sharing, distribution and reproduction in any medium or format, as long as you give appropriate credit to the original author(s) and the source, provide a link to the Creative Commons licence, and indicate if you modified the licensed material. You do not have permission under this licence to share adapted material derived from this article or parts of it. The images or other third party material in this article are included in the article's Creative Commons licence, unless indicated otherwise in a credit line to the material. If material is not included in the article's Creative Commons licence and your intended use is not permitted by statutory regulation or exceeds the permitted use, you will need to obtain permission directly from the copyright holder. To view a copy of this licence, visit <http://creativecommons.org/licenses/by-nc-nd/4.0/>.

© The Author(s) 2024